REGULAR ARTICLE

blood advances

A role for IL-34 in osteolytic disease of multiple myeloma

Muhammad Baghdadi,[1] Kozo Ishikawa,[1] Sayaka Nakanishi,[1] Tomoki Murata,[1] Yui Umeyama,[1] Takuto Kobayashi,[1] Yosuke Kameda,[1] Hiraku Endo,[1] Haruka Wada,[1] Bjarne Bogen,[2] Satoshi Yamamoto,[3] Keisuke Yamaguchi,[3] Ikumi Kasahara,[3] Hiroshi Iwasaki,[4] Mutsumi Takahata,[4] Makoto Ibata,[4] Shuichiro Takahashi,[5] Hideki Goto,[5] Takanori Teshima,[5] and Ken-ichiro Seino[1]

[1]Division of Immunobiology, Institute for Genetic Medicine, Hokkaido University, Sapporo, Japan; [2]K. G. Jebsen Centre for Influenza Vaccine Research, University of Oslo, Oslo, Norway; [3]Department of Hematology, Sapporo City General Hospital, Sapporo, Japan; [4]Department of Hematology, Sapporo Kosei General Hospital, Sapporo, Japan; and [5]Department of Hematology, Faculty of Medicine, Hokkaido University, Sapporo, Japan

Key Points

- IL-34 expression can be observed in MM cells.
- IL-34 may have a pathological role in accelerating MM-induced osteoclast formation and increasing the severity of bone lesions.

Multiple myeloma (MM) is a hematological malignancy that grows in multiple sites of the axial skeleton and causes debilitating osteolytic disease. Interleukin-34 (IL-34) is a newly discovered cytokine that acts as a ligand of colony-stimulating factor-1 (CSF-1) receptor and can replace CSF-1 for osteoclast differentiation. In this study, we identify IL-34 as an osteoclastogenic cytokine that accelerates osteolytic disease in MM. IL-34 was found to be expressed in the murine MM cell line MOPC315.BM, and the expression of IL-34 was enhanced by stimulation with proinflammatory cytokines or by bone marrow (BM) stromal cells. MM-cell–derived IL-34 promoted osteoclast formation from mouse BM cells in vitro. Targeting *Il34* by specific small interfering RNA impaired osteoclast formation in vitro and attenuated osteolytic disease in vivo. In BM aspirates from MM patients, the expression levels of IL-34 in $CD138^+$ populations vary among patients from high to weak to absent. MM cell–derived IL-34 promoted osteoclast formation from human $CD14^+$ monocytes, which was reduced by a neutralizing antibody against IL-34. Taken together, this study describes for the first time the expression of IL-34 in MM cells, indicating that it may enhance osteolysis and suggesting IL-34 as a potential therapeutic target to control pathological osteoclastogenesis in MM patients.

Introduction

Bone lesions represent a prominent feature of multiple myeloma (MM) that significantly impact the quality of life of MM patients.[1-4] Understanding the biology of osteoclasts has helped to develop therapeutic strategies to control bone destruction in MM patients, represented mainly by targeting the bone remodeling ligand, receptor activator of nuclear factor κ-B ligand (RANKL).[1-4] Unfortunately, treatment with RANKL inhibitors is associated with several serious complications, such as joint and muscle pain, increased risk of infection, uncontrolled serum calcium, jaws osteonecrosis, and hypersensitivity allergic reactions.[1-4] Thus, identifying additional therapeutic targets with fewer side effects may help to reduce the suffering of MM patients due to osteolysis.

In addition to RANKL, colony-stimulating factor-1 (CSF-1) receptor (CSF-1R)-mediated signaling is critical for osteoclast differentiation and activation.[5] CSF-1R is a tyrosine kinase transmembrane receptor that acts through binding to 2 distinct ligands: CSF-1 and interleukin-34 (IL-34). IL-34 was identified in a systematic functional screening of the extracellular proteome as a protein that binds to the extracellular domain of CSF-1R, which promotes monocyte survival and proliferation.[6] IL-34 and CSF-1 share similar functions, regulating myeloid lineage differentiation, proliferation, and survival.[7,8] In normal conditions, IL-34 acts as a tissue-specific ligand of CSF-1R in 2 major sites: the skin and

Submitted 23 April 2018; accepted 9 January 2019. DOI 10.1182/bloodadvances.2018020008.

The full-text version of this article contains a data supplement.

brain, secreted by keratinocytes and neurons, and mediating the development and maintenance of Langerhans cells and microglia, respectively.[7,8] In disease, IL-34 has been suggested to play essential roles in the pathological mechanisms of autoimmune disorders, inflammation, infection, and cancer.[7,8]

As a ligand of CSF-1R, IL-34 is capable of inducing osteoclast differentiation and activation when combined with RANKL.[9-12] As suggested by in vitro evidence, IL-34 modulates cell adhesion, differentiation, fusion, and resorbing activity in osteoclast precursors, whereas RANKL is dedicated to osteoclast fusion, activation, and survival.[9-12] In studies on knockout mice, the deficiency of CSF-1R (*Csf1r*$^{-/-}$) results in a severe osteopetrosis phenotype and systemic depletion of macrophages.[13] In contrast, bone malformations observed in *Csf1r*$^{-/-}$ mice were not detectable in *Il34*-deficient (*Il34*$^{LacZ/LacZ}$) mice, suggesting that the role of IL-34 in normal osteoclastogenesis is little.[14,15] On the other hand, accumulating evidence suggests an important role of IL-34 in pathological osteoclastogenesis, represented by supporting RANKL-induced osteoclastogenesis by enriching the microenvironment with bone-resorbing osteoclasts, resulting in bone lesions such as in rheumatoid arthritis and giant cell tumors.[10-12]

As a ligand of CSF-1R, IL-34 is expected to play important protumorigenic roles at the tumor microenvironment (TME).[16-23] In cancer patients, the expression level of IL-34 varies among cancer patients from high to weak to absent, and correlates with disease progression and poor prognosis when highly expressed.[22] In this regard, little is known regarding the role of IL-34 in hematological malignancies. As an osteoclastogenic cytokine, we expected a potential role for IL-34 in the pathogenesis of MM. In this study, we explore the possible involvement of IL-34 in MM pathogenesis in a murine model of MM and in clinical samples from MM patients.

Materials and methods

Cell lines

The murine MOPC315.BM cell line was cultured in RPMI 1640 plus GlutaMAX-I (Gibco) supplemented with 10% fetal bovine serum (FBS; Sigma), 1% minimum essential medium nonessential amino acids 100× (Nacalai Tesque), 1% sodium pyruvate (Nacalai Tesque), 0.005% 1 M l-thioglycerol solution (Sigma-Aldrich), penicillin (100 IU/mL)/streptomycin (100 μg/mL; Nacalai Tesque), and Plasmocin (InvivoGen). Human myeloma cell lines (KMS-11, OPC, OPM-2, and U226B1) were kindly provided by Masahiro Abe (Department of Hematology, Graduate School of Medicine, Tokushima University, Tokushima, Japan) and cultured in RPMI 1640 medium supplemented with 5% FBS. The IM-9 cell line was purchased from the Japanese Collection of Research Bioresources (JCRB) Cell Bank. The Lenti-X 293T cell line was purchased from TaKaRa. All cells were cultured at 37°C in a humidified incubator supplemented with 5% CO_2.

Clinical samples

Human diagnostic bone marrow (BM) aspirates from 15 MM patients were obtained from the Department of Hematology of Sapporo City General Hospital, Sapporo Kosei General Hospital, and Hokkaido University Hospital (Sapporo, Japan). All participants gave written informed consent, and all experiments were approved by the institutional review boards of Hokkaido University Hospital (approval no. 018-0076) per the Declaration of Helsinki.

Cell stimulation

MOPC315.BM cells were stimulated for 7 days with recombinant mouse IL-1β (BioLegend), IL-6 (BioLegend), transforming growth factor β (TGFβ; R&D Systems), or tumor necrosis factor α (TNFα; BioLegend) (100 ng/mL). Protein levels of IL-34 in the supernatants were measured using a LEGEND MAX Mouse IL-34 ELISA Kit (BioLegend). Human MM cell lines were stimulated for 7 days with recombinant human IL-1β (BioLegend), IL-6 (BioLegend), TGFβ (BioLegend), or TNFα (BioLegend). Protein levels of IL-34 in the supernatants were measured using Human IL-34 ELISA MAX Deluxe (BioLegend).

Generation of *Il34* knockdown MOPC315.BM cell line

Firefly luciferase (Luc) lentiviral particles were generated by transfecting Lenti-X 293T cells with psPAX2 (Addgene), pMD2.5 (Addgene), and pLenti-PGK-V5-Luc Neo (W632-2) using TransIT-X2 transfection reagent (Miru). Supernatants containing lentiviral particles were collected and used to infect MOPC315.BM cells, which were then continuously selected by G418 (500 μg/mL). Then, gene silencing of *Il34* was performed using lentivirus-mediated delivery of *Il34*-specific small interfering RNA (siRNA; Applied Biological Materials). Stable cells expressing *Il34*-specific siRNA (MOPC315.BM^{Il34KD}) or scramble siRNA (MOPC315.BM^{Control}) were selected with puromycin (2.5 μg/mL), and green fluorescent protein (GFP) expression was confirmed periodically by fluorescence microscope. Knockdown efficiency and relative *Il34* messenger RNA (mRNA) expression were determined by quantitative reverse transcription polymerase chain reaction (qRT-PCR). Comparable bioluminescence signals between the 2 cell lines were confirmed each time before injecting into mice. Cell proliferation was evaluated using the MTT Cell Assay kit (BioAssay Systems). M315 myeloma protein was measured as previously described.[24]

Quantitative real-time PCR

Total RNA was extracted using a PureLink RNA Micro kit (Invitrogen) and used for complementary DNA (cDNA) synthesis using ReverTraAce qPCR RT Master Mix (TOYOBO). cDNA products were used to amplify target genes using a KAPA SYBR Fast qPCR kit (Nippon Genetics). PCR and data analysis were performed on a StepOne real-time PCR machine (Applied Biosystems). Primers sequences are listed in supplemental Table 1.

Flow cytometry

Plasma cells were purified from mouse BM cells as CD138^{+} (BioLegend), CD45R^{Low} (BioLegend), and CD19^{-} (BioLegend) populations. B lymphocytes were purified from mouse splenocytes as CD45^{+} (BioLegend) and CD19^{+} populations. MOPC315.BM cells were purified from mouse BM cells as GFP^{+}CD138^{+} populations. Live/dead cell analysis was performed using Ghost Dye TM Violet 510 (TOMBO). Cells were sorted using a SH800 Cell Sorter (Sony Biotechnology).

Cytokine/chemokine concentrations in the supernatants of MM–BM stromal cell (BMSC) coculture were measured using a LEGENDplex Mouse Th Cytokine Panel (13-plex) and LEGENDplex Mouse Cytokine Panel 2 (13-plex) (BioLegend).

In clinical samples, BM cells were stained for CD19 (BioLegend) and CD138 (BioLegend) or isotype controls (BioLegend). Then, intracellular staining of IL-34 was performed using specific

anti-IL-34 antibody (Novus Biologicals) compared with an isotype control (BioLegend). Fc blocking was performed using human TruStain FcX (BioLegend). Samples were run on a BD FACSCanto II flow cytometer and data were analyzed using FlowJo software.

Evaluation of MM cell–induced osteoclast formation

Mouse BMSCs were collected from an adherent culture of whole BM cells, and cocultured with MM cells (MOPC315.BM^{Control} or MOPC315.BM^{Il34KD}) directly or separately using a Transwell culture plate (Corning Incorporated) for 7 days. To evaluate the impact of MM-BMSC interaction on osteoclast formation, MM-BMSCs were cultured at the upper chamber of a Transwell culture plate, whereas BM cells were seeded in the lower chamber. In other experiments, MM-BMSCs were cocultured directly with BM cells.

In clinical samples, MM cells with high or low expression of IL-34 were cultured at the upper chamber of a Transwell culture plate, whereas human CD14$^+$ monocytes purified from the peripheral blood mononuclear cells of healthy donors (Miltenyi Biotec) were seeded in the lower chamber. In each case, recombinant human RANKL (100 ng/mL; BioLegend) alone or combined with a neutralizing anti–IL-34 antibody (10 μg/mL; R&D Systems) or isotype control (R&D Systems) were added to the culture.

Osteoclast formation was evaluated by qRT-PCR or tartrate-resistant acid phosphatase (TRAP) staining (TRACP and ALP double-stain kit; TaKaRa).

Mouse experimental model

Six- to 8-week-old female wild-type BALB/c mice (SLC) were IV injected with 2×10^5 Luc$^+$GFP$^+$ MOPC315.BM cells (MOPC315.BM^{Control} or MOPC315.BM^{Il34KD}).

For in vivo bioluminescence imaging, mice were IV injected with A-Luciferin (150 mg/kg dissolved in phosphate-buffered saline [PBS]; Avidin Ltd) and images were acquired from 5 to 15 minutes using IVIS Spectrum Imaging Systems (Spectrum-FL-TKHD; Caliper Life Sciences Ltd). Data were analyzed using Living Image software (Caliper Life Sciences Ltd) compared with control (tumor-free control mice administered with A-luciferin). Bioluminescence signals were quantified using average photons per second per centimeter-squared per steradian with the respective area on the tumor-free control mice subtracted.

Transmission micro CT (μCT) analysis was performed using the Latheta LCT200 system (Hitachi Aloka Medical). Cross-sectional scan slices (24-μm thick) of the skull, vertebra, and femur were obtained. Selected areas of the skull and vertebra were scanned under general anesthesia (medetomidine/midazolam/butorphanol: 0.3/4.0/5.0 mg/kg) at day 45 postinjection. Femurs were explanted and fixed in 4% paraformaldehyde before analyzing with a μCT scan. Regions of interest were accurately determined from the cross-sectional scout views. For bone structural quantitative analysis, bone mineral density (milligrams per meters-cubed) and mineral volume (milligrams) of trabecular and cortical bones were individually calculated using the system's software (Latheta, LCT200; ALOKA). μCT-generated 3-dimensional images were reconstructed to an isotropic voxel size of 24 μm by using Amira 5.4.1 software (Maxnet Co).

In some experiments, blood samples were collected from the retro-orbital sinus of mice once in 2 weeks. Serum Ca^{2+} was measured using Calcium Assay Kit LS (MG Metallogenics). Protein levels of IL-34 in the BM fluid (BMF) were measured using Human IL-34 ELISA MAX Deluxe (BioLegend). All experiments were approved by the Animal Care Committee of Hokkaido University (approval no. 15-0101).

Statistics

Data are shown as mean ± standard deviation. Statistical significance was determined via the 2-tailed Student *t* test. Differences were considered statistically significant when $P < .05$.

Results

IL-34 expression in a murine model of MM

To evaluate the possible role of IL-34 in MM pathogenesis, we used a mouse MM cell line, MOPC315.BM, which replicates many characteristics of human MM.[24] First, we examined whether IL-34 is expressed in MOPC315.BM cells. At the mRNA level, *Il34* could be detected in MOPC315.BM cells and this expression was higher than that of normal plasma cells (CD19$^-$CD138$^+$ cells) (Figure 1A-B) or B lymphocytes (CD19$^+$CD138$^-$ cells) (supplemental Figure 1A-B). The nucleotide sequence of the PCR product was identical to the *Il34* sequence (isoform 1) registered at the National Center for Biotechnology Information (NCBI) database (supplemental Figure 1C). At the protein level, IL-34 could be detected at low concentrations in the supernatants of MOPC315.BM cells, which were enhanced upon exposure to stimulation with cytokines that have functional importance at the BM microenvironment (BME) such as IL-1β, IL-6, TGFβ, and TNFα (Figure 1C; supplemental Figure 1D). Thus, we expected that the expression of IL-34 in MOPC315.BM cells would be changed at the BME. To confirm the expression of *Il34* in MOPC315.BM cells in vivo, BALB/c mice were IV injected with MOPC315.BM labeled with firefly Luc and GFP. Then, the expression of *Il34* was compared between Luc$^+$GFP$^+$ MOPC315.BM cells purified directly from the BM of femurs or cultured in vitro. Interestingly, we found that the expression of *Il34* was significantly enhanced in MOPC315.BM cells isolated from femurs compared with in vitro culture (Figure 1D). Next, we aimed to measure the protein level of IL-34 in the BMF collected from femurs. The homing of MOPC315.BM cells to the BM showed considerable individual variability as unveiled by bioluminescence imaging and flow cytometry analysis (Figure 1E). Interestingly, high frequencies of MOPC315.BM cells in the BM correlated positively with strong luciferase bioluminescent signals (Figure 1F) and elevated levels of IL-34 (Figure 1G). The average of IL-34 concentrations was statistically higher in mice challenged with MOPC315.BM cells (903.98 ± 373.28 pg/mg) compared with healthy controls (462.63 ± 210.44 pg/mg) (data not shown; $P = .004$). Collectively, these results suggest that IL-34 expression can be detected in MOPC315.BM cells, and that this expression is enhanced at the BME.

Establishment of *Il34*^{KD} MOPC315.BM cells

To gain insight into the possible pathological role of IL-34 in the MOPC315.BM model, we next used a lentiviral system to generate MOPC315.BM cell lines that stably express *Il34*-specific siRNA or scramble siRNA. The knockdown efficiency was >80% in MOPC315.BM cells expressing *Il34*-specific siRNA compared with control (Figure 2A). The cellular morphology, proliferation, and production levels of M315 myeloma protein were comparable

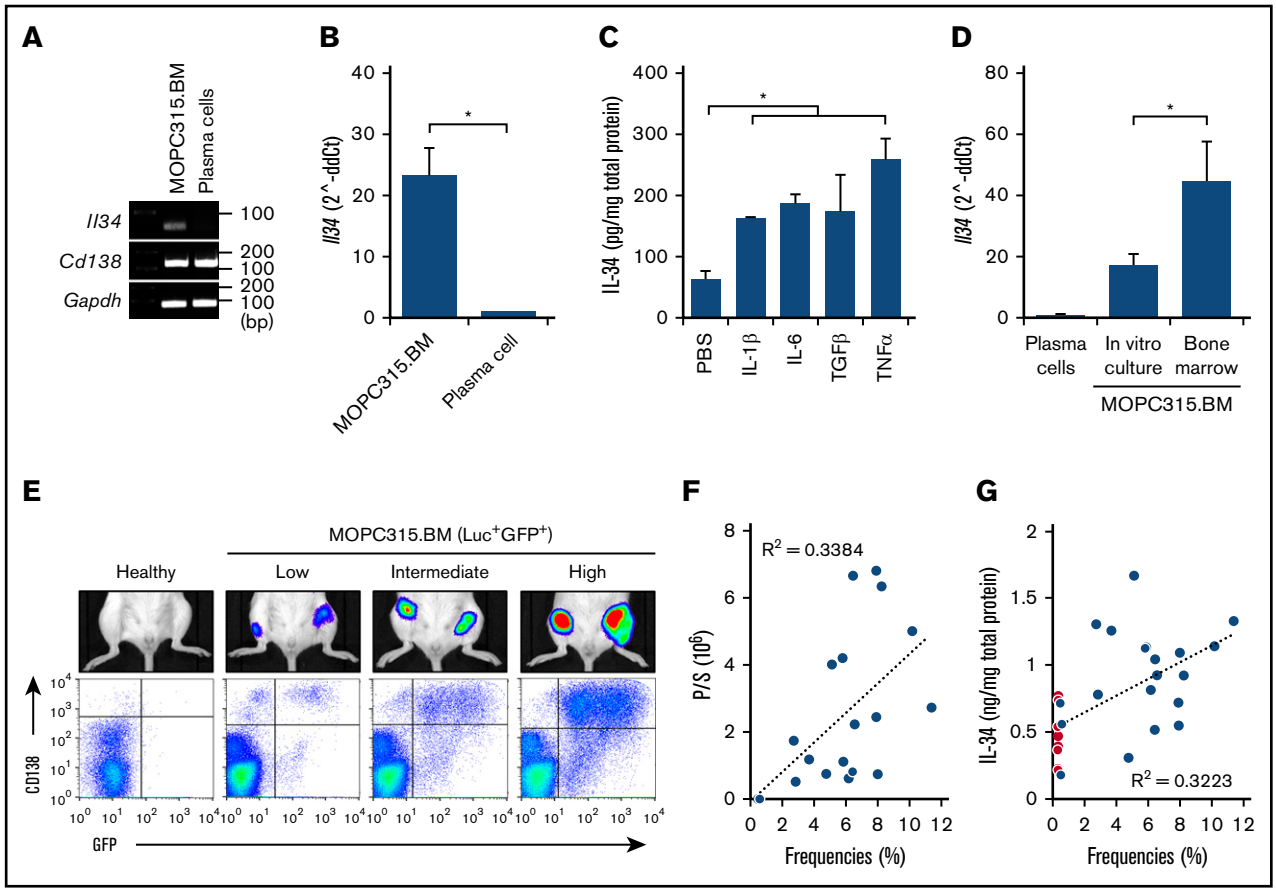

Figure 1. IL-34 expression in MOPC315.BM cells. (A) PCR analysis of *Il34*, *Cd138*, and *Gapdh* expression in MOPC315.BM cells compared with normal plasma cells. (B) Relative expression of *Il34* expression in MOPC315.BM cells compared with normal plasma cells (normalized to *Gapdh*). (C) Enzyme-linked immunosorbent assay (ELISA) measurement of IL-34 in the supernatants of MOPC315.BM cells stimulated for 7 days with IL-1β, IL-6, TGFβ, or TNFα (100 ng/mL) compared with PBS. (D) qRT-PCR analysis of *Il34* expression in MOPC315.BM cells purified directly from the BM (day 30 after IV injection) or cultured in vitro compared with plasma cells (normalized to *Gapdh*). (E) Individual variability of MOPC315.BM cells homing to the bones. Top panel, The bioluminescence signals in representative BALB/c mice challenged with Luc^+ GFP^+ MOPC315.BM cells compared with healthy controls. Bottom panel, Populations of $CD138^+GFP^+$ cells (MOPC315.BM) in the BM of femurs as analyzed by flow cytometry (day 30 after IV injection). (F) The correlation between frequencies of Luc^+GFP^+ MOPC315.BM cells with bioluminescence signals in femurs. (G) The correlation between frequencies of Luc^+GFP^+ MOPC315.BM cells with protein levels of IL-34 in the BMF of femurs. Red dots indicate levels of normal IL-34 levels in healthy controls. Data are mean ± standard error of the mean (SEM); $*P < .05$. ddCt, delta-delta cycle threshold; P/S, photon/second.

between $MOPC315.BM^{Control}$ and $MOPC315.BM^{Il34KD}$ cells (Figure 2B-D). Next, both cell lines were IV injected into BALB/c mice to examine the knockdown efficiency of *Il34* in vivo. The expression of *Il34* was efficiently suppressed in $MOPC315.BM^{Il34KD}$ cells collected directly from the BM as compared with control at day 30 or day 45 postinjection (Figure 2E). Additionally, both cell lines showed similar homing to the bones and spleen, indicating that this process is also IL-34 independent (Figure 2E, G). Thus, we next focused on the possible involvement of IL-34 as an osteoclastogenic cytokine in MM-induced bone lesions.

IL-34 promotes MM-induced osteoclastogenesis in vitro

The BME consists of various molecular and cellular components that play critical roles in the pathogenesis of MM. As an osteoclastogenic cytokine, IL-34 binds to CSF-1R and induces osteoclast differentiation and bone resorption from BM cells when combined with RANKL. In the BME where MOPC315.BM cells have settled within, *Csf1r*, *Rankl*, and *Il34* show relatively high expression in the $CD45^+$ myeloid compartment, $CD45^-$ stromal compartment, and MM (MOPC315.BM) cells, respectively (Figure 3A). Previous reports suggested that the adhesion of MM cells to BMSCs induces the secretion of various factors that contribute to osteoclast formation and activation.[25,26] Thus, we hypothesized that the enhancement of *Il34* expression in MOPC315.BM cells at the BME might be affected by the interaction between BMSCs and MM cells. To evaluate this hypothesis, BMSCs were isolated from the BM of mice and cocultured with MOPC315.BM cells. As expected, the supernatant of BMSC-$MOPC315.BM^{Control}$ coculture was enriched with several cytokines including IL-3, IL-6, TNFα, and, importantly, IL-34 (Figure 3B). RT-PCR analysis unveiled that the expression levels of *Il3* and *Il34* were enhanced in MOPC315.BM cells, whereas the expression levels of *Il6*, *Tnfa*, and *Rankl* were enhanced in BMSCs in this coculture (supplemental Figure 2). The enrichment with IL-3, IL-6, and TNFα was similarly observed in the supernatant

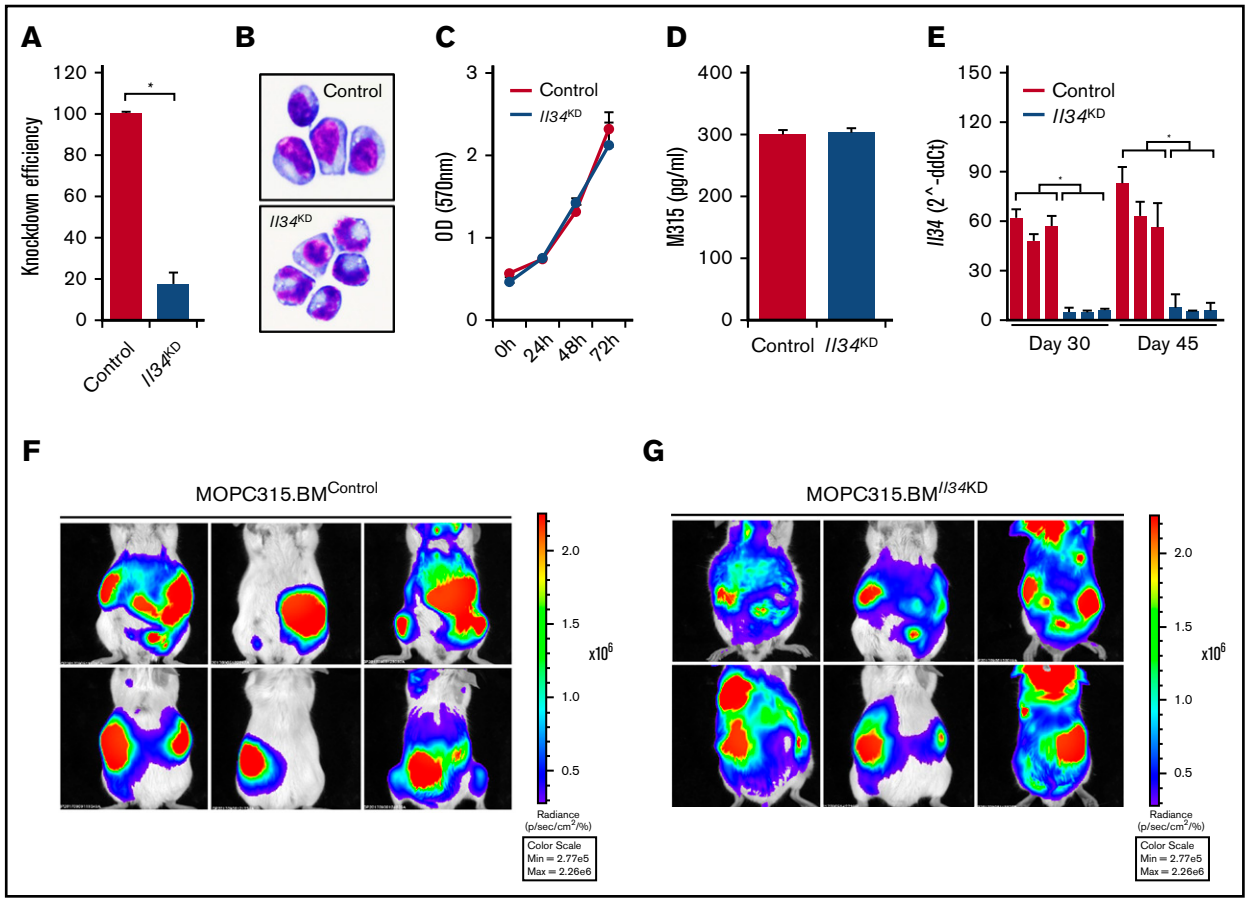

Figure 2. Knocking down *Il34* expression in MOPC315.BM cells. (A) Knockdown efficiency of *Il34* expression in MOPC315.BM cells that stably express *Il34*-specific siRNA compared with control as evaluated by qRT-PCR (control = 100%). (B) Cellular morphology of MOPC315.BM^{Control} (top: hematoxylin and eosin stain; original magnification ×20) or MOPC315.BM^{Il34KD} (bottom: hematoxylin and eosin stain; original magnification ×20) cells. (C) Cell proliferation as compared between MOPC315.BM^{Control} and MOPC315.BM^{Il34KD} cells. (D) ELISA measurement of M315 protein in the supernatants of MOPC315.BM^{Control} or MOPC315.BM^{Il34KD} cell cultures. (E) qRT-PCR analysis of *Il34* expression in MOPC315.BM^{Control} or MOPC315.BM^{Il34KD} cells collected from bones of mice (n = 3) at day 30 or day 45 postinjection (normalized to *Gapdh*). (F-G) Bioluminescence imaging in representative BALB/c mice challenged with MOPC315.BM^{Control} (F) or MOPC315.BM^{Il34KD} cells (G) at day 45 postinjection. Ventral and dorsal views are shown in the top and bottom panels, respectively. Data are mean ± SEM; *$P < .05$. OD, optical density.

of BMSC-MOPC315.BM^{Il34KD} coculture, indicating that this enrichment is IL-34 independent (Figure 3B).

Next, we aimed to evaluate the impact of IL-34 on osteoclast formation in this model. To do so, BMSCs were cultured either alone or with MM cells (MOPC315.BM^{Control} or MOPC315.BM^{Il34KD}) in the upper chamber of a Transwell culture plate, while mouse BM cells that contain osteoclast precursors were cultured in the lower chamber. Notably, the expression levels of osteoclastogenesis-related genes such as *Trap*, *Dc-stamp*, *Oc-stamp*, and *Cathepsin K* were significantly enhanced in BM cells cultured in the presence of BMSC-MOPC315.BM^{Control} cells compared with other groups (Figure 3C). Consistent with this enhancement, BM cells showed efficient differentiation into osteoclasts as featured by a large multinuclear cellular morphology and high positivity for TRAP staining (Figure 3D). On the other hand, osteoclast formation in this model was attenuated by *Il34* deficiency (Figure 3C-D). A similar tendency was also observed in BM cells that were cocultured directly with BMSC-MOPC315.BM^{Control} or BMSC-MOPC315.BM^{Il34KD} cells (data not shown). Together, these results suggest that IL-34 is likely to provide an essential signal that helps to initiate osteoclast differentiation in this model. However, it is worth mentioning here that the osteoclast formation described herein was performed in a well-controlled in vitro culture system and MM-induced osteoclastogenesis can also be affected by several factors available at the BME.

IL-34 promotes MM-induced osteolysis in vivo

Next, we examined the possible involvement of IL-34 in MM-induced osteolysis in vivo. As suggested earlier in text, both MOPC315.BM^{Control} and MOPC315.BM^{Il34KD} cells show similar homing to the bones in mice. In the next experiment, BALB/c mice were IV injected with MOPC315.BM^{Control} or MOPC315.BM^{Il34KD} cells and bone lesions in the skull, distal femur, or spinal cord were evaluated by transmission radiographs in mice that showed similar distribution and comparable luminescence signals of MOPC315.BM^{Control} or MOPC315.BM^{Il34KD} cells in the mentioned regions (supplemental Figure 3). Compared with healthy controls, mice challenged

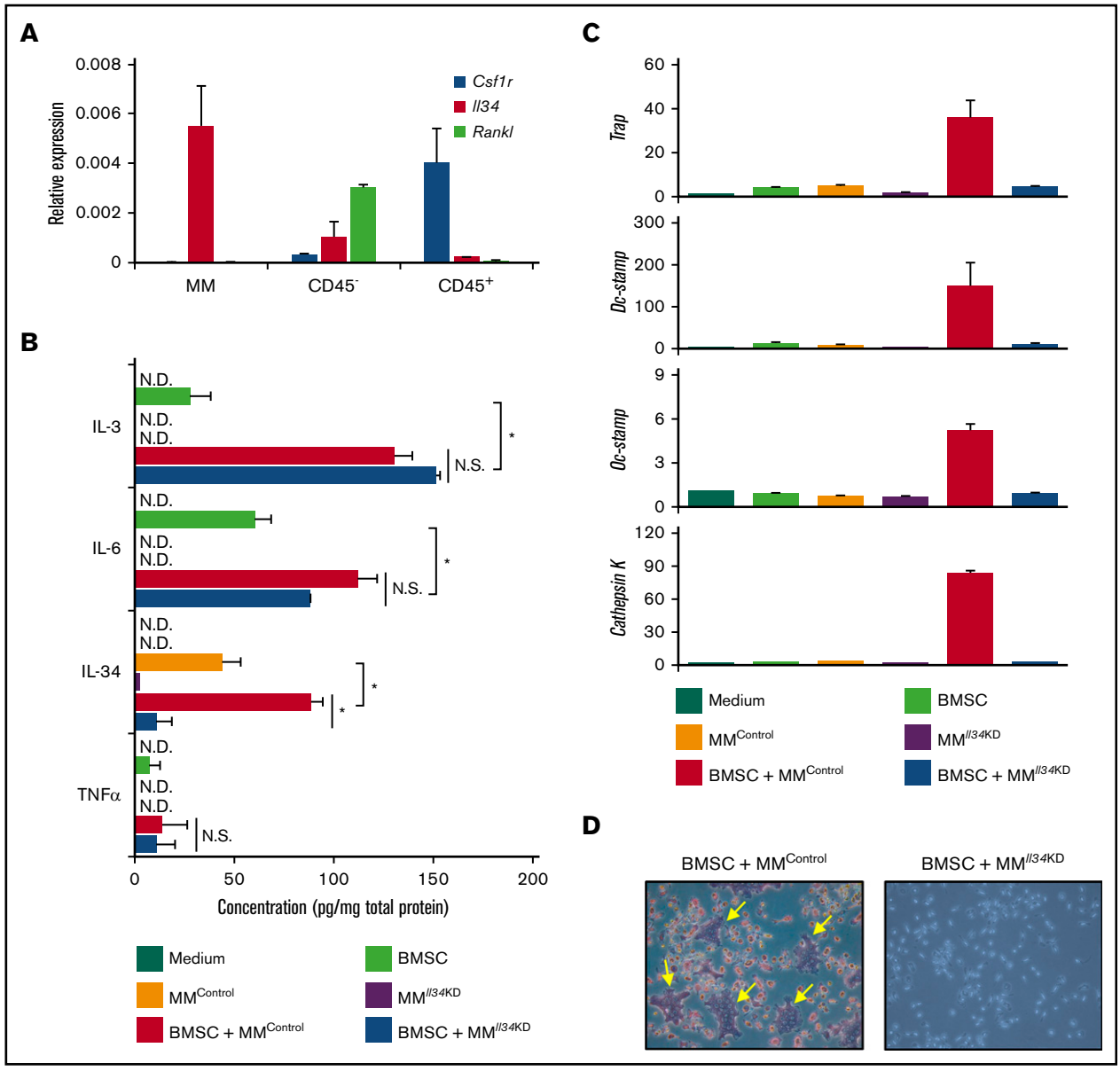

Figure 3. IL-34 accelerates MM-induced osteoclast formation in vitro. (A) Relative expression of *Csf1r*, *Il34*, or *Rankl* mRNA in the CD45$^+$ myeloid compartment, CD45$^-$ stromal compartment, or MOPC315.BM cells (normalized to *Gapdh*). (B) Protein levels of IL-3, IL-6, IL-34, and TNFα in the supernatants of the indicated cultures. (C) qRT-PCR analysis of *Trap*, *Dc-stamp*, *Oc-stamp*, or *Cathepsin K* in BM cells differentiated in the presence of the indicated cultures. (D) Representative photomicrographs (TRAP stain; original magnification ×5) of BM cells differentiated for 10 days in the presence of supernatants of BMSCs-MOPC315.BM^{Control} or BMSCs-MOPC315.BM^{Il34KD} cocultures. Yellow arrows indicate TRAP$^+$ multinucleated cells. Data are mean ± SEM; *$P < .05$. N.D., not determined; N.S., not significant.

with MOPC315.BM^{Control} cells suffered from severe bone lesions associated with decreased bone volumes and mineral densities, which were remarkably attenuated by *Il34* deficiency (Figure 4A-F). Consistent with these results, a significant increase in calcium (Ca^{2+}) in the sera was observed in mice challenged with MOPC315.BM^{Control} compared with MOPC315.BM^{Il34KD} cells (Figure 4G), suggesting a potential role of IL-34 in accelerating MM-induced osteolysis.

IL-34 expression in human MM cells

In addition to mice, several studies have shown that IL-34 activates signaling pathways downstream of CSF-1R in human CD14$^+$ monocytes, resulting in osteoclast formation when combined with RANKL, which was also confirmed in our experiments (supplemental Figure 4).[9-12] As suggested earlier in text, IL-34 may have a potential role in accelerating MM-induced osteolysis in a mouse model. Thus, we finally examined the possible involvement of IL-34 in MM-induced osteolysis in human. In human MM cell lines, IL-34 was detected in the supernatants of IM-9, KMS-11, OPC, OPM-2, and U226B1 upon the exposure to cytokine stimulation such as IL-1β, IL-6, TGFβ, and TNFα (Figure 5A). Next, we examined the expression of IL-34 in CD19$^-$CD138$^+$ cells in BM aspirates collected from a cohort of patients diagnosed with MM (n = 15; supplemental Table 2). Importantly, IL-34 staining was strong in 20% (3 of 15), weak in

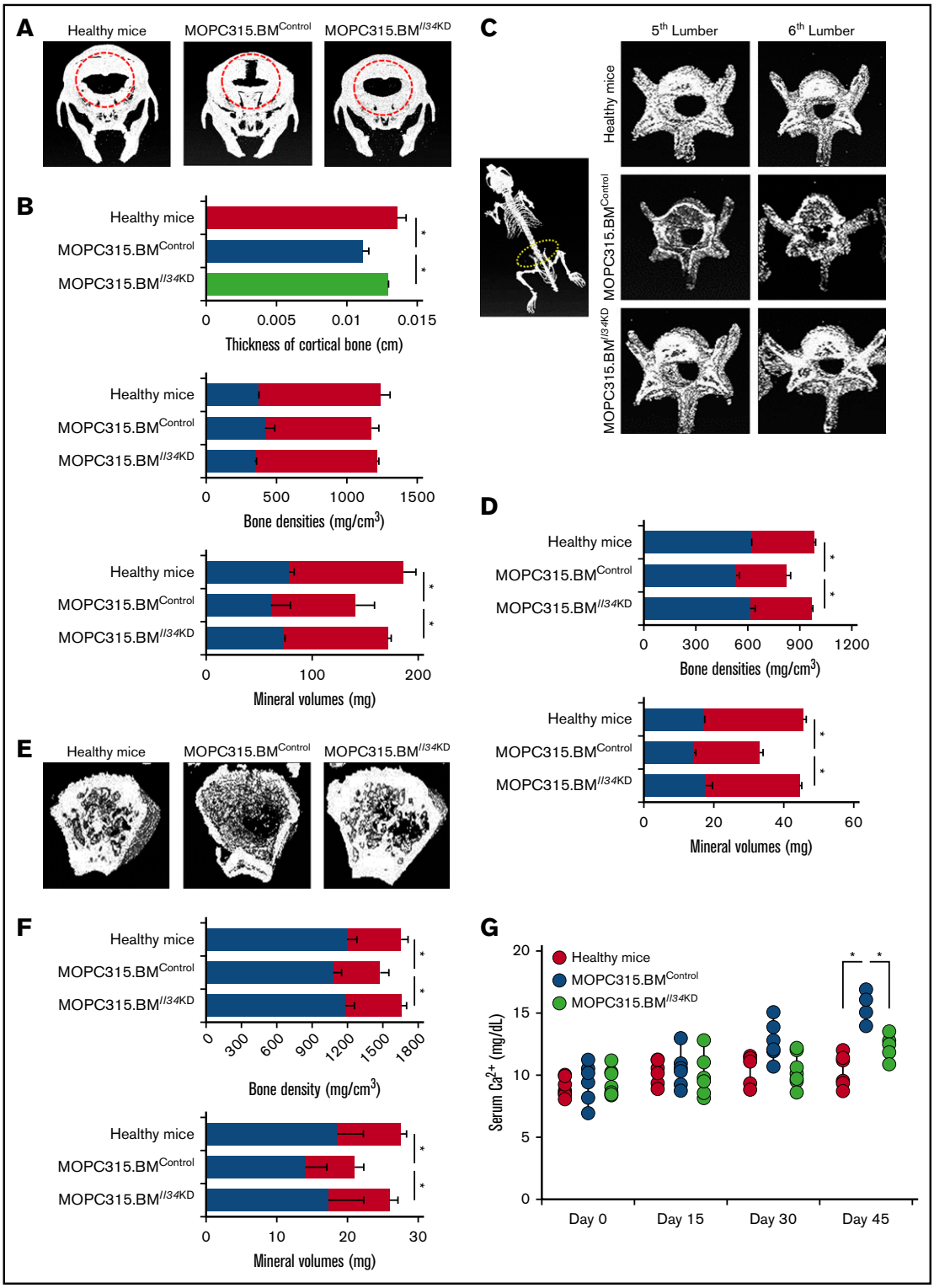

Figure 4. IL-34 accelerates MM-induced osteolysis in mice. (A) Transmission radiographs of the skull of mice IV injected with MM cells (MOPC315.BM^{Control} or MOPC315.BM^{Il34KD}) at day 45 postinjection, compared with age-matched healthy controls. Red circles refer to regions with severe bone lesions. (B) Quantitation of cortical bone thickness (centimeters), bone densities (milligrams per centimeter-cubed), and mineral volumes (milligrams) of regions described in panel A. (C) Transmission radiographs of the fifth and sixth lumbar vertebrae of mice described in panel A. (D) Quantitation of bone densities (milligrams per centimeter-cubed) and mineral volumes (milligrams) of regions described in panel C. (E) Transmission radiographs of femurs of mice described in panel A. (F) Quantitation of bone densities (milligrams per centimeter-cubed) and mineral volumes (milligrams) of regions described in panel E. Blue bars, cortical structures; red bars, trabecular structures. (G) Measurement of serum Ca^{2+} levels in mice described in panel A at the indicated days after injection. Data are mean ± SEM; *$P < .05$.

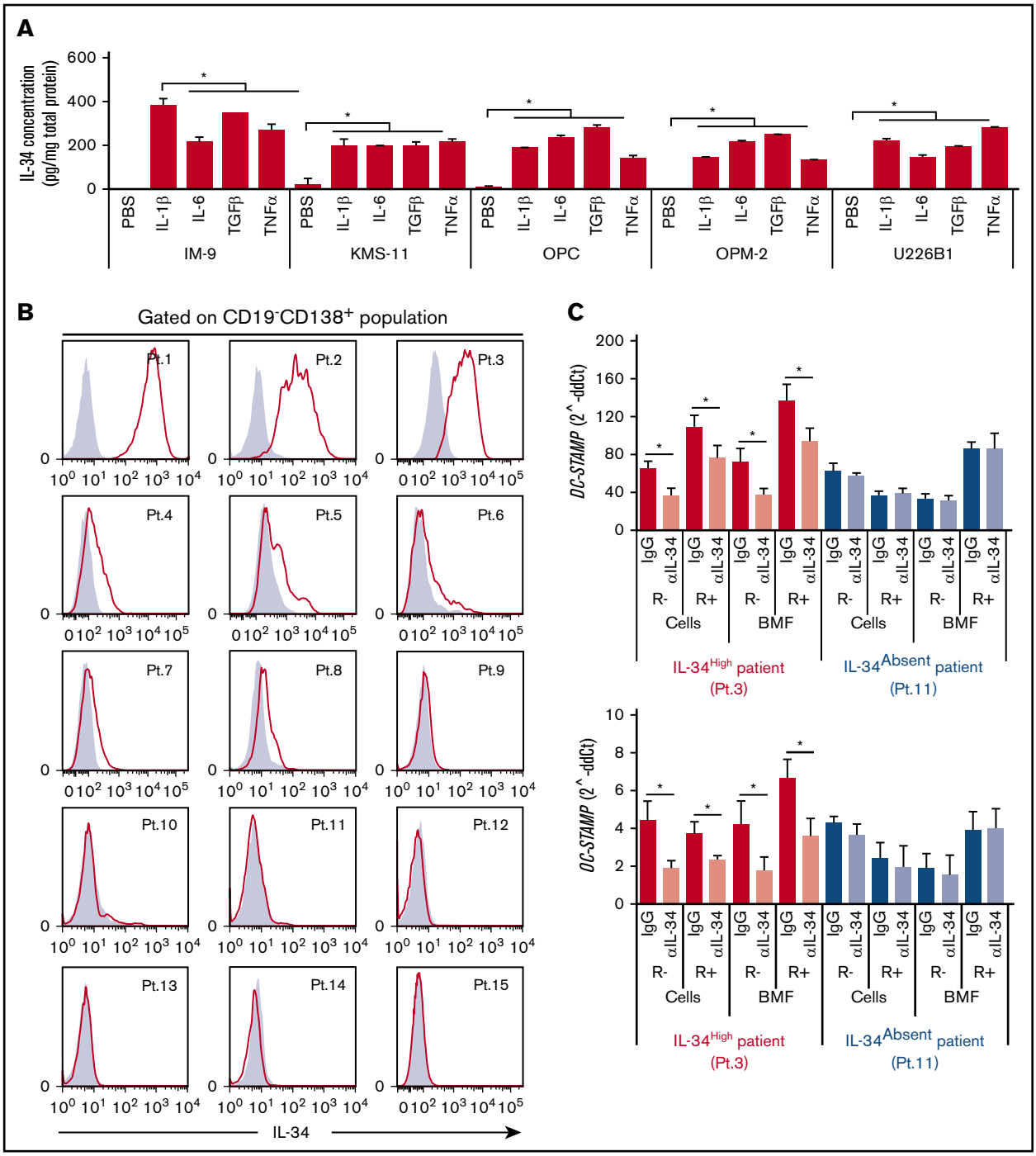

Figure 5. Human MM cell–derived IL-34 accelerates osteoclast formation. (A) ELISA measurement of IL-34 in the supernatants of IM-9, KMS-11, OPC, OPM-2, and U226B1 human MM cell lines stimulated with IL-1β, IL-6, TGFβ, or TNFα (100 ng/mL) for 7 days. (B) Intracellular staining of IL-34 in CD19$^-$CD138$^+$ populations in BM aspirates collected from MM patients (Pt.). Gray histogram, isotype; red line, IL-34. (C) Fold induction of *DC-STAMP* (top) or *OC-STAMP* (bottom) expression in human CD14$^+$ monocytes cocultured with MM cells or stimulated with BMF from IL-34^{High} or IL-34^{Absent} patients in the presence or absence of RANKL (referred to as R). A neutralizing antibody against IL-34 (αIL-34) or an isotype control antibody (immunoglobulin G [IgG]) was added to the culture. Unstimulated monocytes were considered as 1. Data are mean ± SEM; *$P < .05$.

33.3% (5 of 15), and absent in 46.7% (7 of 15) of cases (Figure 5B). Consistent with this, IL-34 could be detected in the BMF of patients who showed high expression of IL-34 (121.95 ± 47.5 pg/mg), whereas it was undetectable in other samples (data not shown). Next, we examined the impact of MM cell–derived IL-34 on osteoclast formation. To do so, human CD14$^+$ monocytes were purified from healthy donors and cultured in the lower chamber of a Transwell culture system in the presence or absence of RANKL, whereas

primary MM cells with high or absent expression of IL-34 were cultured in the upper chamber. In other experiments, human $CD14^+$ monocytes were similarly stimulated with the BMF of patients who showed high or absent expression of IL-34 in the presence or absence of RANKL. In both cases, a neutralizing antibody against IL-34 or an isotype control antibody was added to the culture. Interestingly, $CD14^+$ monocytes showed enhanced expression levels of osteoclastogenesis-related genes such as *DC-STAMP* and *OC-STAMP* in all samples, which were further enhanced by adding RANKL to the culture (Figure 5C). A higher baseline was observed in $IL\text{-}34^{High}$ compared with $IL\text{-}34^{Absent}$ patients (Figure 5C). Furthermore, anti–IL-34 neutralizing antibody suppressed the induction of *DC-STAMP* and *OC-STAMP* in monocytes cultured in the presence of cells or stimulated with BMF from $IL\text{-}34^{High}$ patients (Figure 5C). Similarly, frequencies of $TRAP^+$ and multinuclear cells were higher in monocytes cultured in the presence of MM cells or BMF from $IL\text{-}34^{High}$ patients, which were decreased by anti–IL-34 neutralizing antibody (supplemental Figure 5). Together, these results suggest a possible involvement of MM cell–derived IL-34 in accelerating osteoclast formation at the BME. This may be supported by clinical data that showed bone lesions in all $IL\text{-}34^{High}$ patients (3 of 3; 100%) compared with $IL\text{-}34^{Low}$ patients (2 of 5; 40%) or $IL\text{-}34^{Absent}$ patients (3 of 7; 42.9%) (supplemental Table 2). Thus, when expressed, IL-34 appears to be involved in osteoclast formation, perhaps enhancing bone lesion in MM patients. It is worth mentioning here that due to the small number of MM patients in this cohort, further analysis on larger cohorts of MM patients is needed in future works to strengthen this conclusion.

Discussion

In this report, we described a novel pathological role for IL-34 expressed by MM cells in promoting osteoclast-mediated bone destruction. The biological function of IL-34 as an osteoclastogenic cytokine has been described previously by several reports that showed the capability of IL-34 of inducing osteoclast formation by activating CSF-1R in its precursors in mouse and human.[9-12] Furthermore, IL-34 has been suggested to promote RANKL-induced pathological osteoclastogeneses such as in rheumatoid arthritis and giant cell tumors.[10-12] In cancer, accumulating evidence has suggested that IL-34 tends to act as a protumorigenic factor at the TME because the expression of IL-34 is frequently accompanied with tumor progression, metastasis, angiogenesis, immunosuppression, and therapeutic resistance.[16-23] Clinically, IL-34 expression in cancer varies among patients, such as in osteosarcoma, malignant pleural mesothelioma, hepatocarcinoma, colon cancer, and lung cancer.[16-23] In this regard, little is known about the expression of IL-34 in hematological malignancies, except for a recent study by Komohara et al that described the expression of IL-34 in adult T-cell leukemia/lymphoma.[27] Similarly, we found here that the expression of IL-34 can be observed in MM cells and varies among MM patients, showing high levels in some cases but being absent in others. In the murine MOPC315.BM MM model, we found that IL-34 importantly contributes to MM-induced osteolytic disease. When expressed, IL-34 is suggested to promote osteoclastogenesis in MM cells.

Through a complex signaling network that involves various types of cells and molecules, IL-34 plays important biological and pathological roles at the site of secretion. Several stimuli can induce or enhance IL-34 expression such as proinflammatory cytokines, pathogen-associated molecular patterns, infections, chemical stressors, and tissue injuries.[7,8,28] On the other hand, IL-34 has the capability of enhancing the expression of several cytokines, chemokines, and metalloproteases in a wide range of cells.[7,8,28] In our experiments, we found that the expression of IL-34 in MM cells can be regulated by cytokines that have functional importance at the BME such as IL-1β, IL-6, TGFβ, and TNFα.[5] Additionally, we also found that IL-34 expression is enhanced in a coculture of MM-BMSCs together with other osteoclast-activating factors. Thus, the expression of IL-34 in MM cells may be largely affected by the cellular and molecular components of the BME where the MM cells have settled within. Furthermore, the induction of IL-34 in MM cells can be possibly mediated by certain oncogenic mutations that activate signaling pathways resulting in the expression of a wide range of cytokines and chemokines.[29-31] In this regard, it is of great interest to examine the impact of oncogenic mutations and other epigenetic changes on IL-34 expression in MM cells in future studies.

Several cytokines play important roles in the maintenance of bone homeostasis.[5] For example, TNFα and IL-6 promote osteoclast differentiation, whereas interferon β and IL-12 downregulate osteoclast formation.[5] IL-34 acts as an osteoclastogenic cytokine that binds to CSF-1R and induces osteoclast differentiation and bone resorption when combined with RANKL.[9-12] Because osteoclast differentiation is regulated by a complex network of osteoclastogenic antiosteoclastogenic cytokines, the pathological osteoclast differentiation in MM patients is not restricted to IL-34 but is expected to be highly accelerated in the existence of this cytokine.

Based on knockout studies in mice, osteopetrosis is observed only in the case of CSF-1 and CSF-1R but not IL-34 deficiency, indicating that bone remodeling depends mainly on the CSF-1/CSF-1R axis under physiological conditions. Considering its high affinity for CSF-1R, IL-34 may act as a strong competitor of CSF-1 when secreted to the BME by MM cells, which disrupts the balance of osteoclast/osteoblast activities toward highly activated bone-resorbing osteoclasts.[14,15] In addition to its broadside effects, targeting of RANKL results in impaired osteoclast function at the systemic level.[32-34] In contrast, targeting of IL-34 may help to abrogate the excessive enhancement of osteoclasts by MM cells. Thus, when expressed, IL-34 may have therapeutic potential to control bone disease in MM. In summary, we described here for the first time the expression of IL-34 in MM cells and suggest IL-34–mediated acceleration of MM-induced osteoclast formation and severity of bone lesions.

Acknowledgments

The authors acknowledge Masahiro Abe (Department of Hematology, Tokushima University, Tokushima, Japan) for providing human MM cell lines, and Rei Okabe (Division of Immunobiology, Hokkaido University, Sapporo, Japan) for academic assistance.

This work was supported partly by the Japan Agency for Medical Research and Development (AMED), the Grant for Joint Research Program of the Institute for Genetic Medicine (Hokkaido University), a Grant-in-Aid for Young Scientists (JSPS KAKENHI; grant no. JP:18K15261), and the Japan Leukemia Research Fund.

Authorship

Contribution: M.B., K.I., S.N., T.M., Y.U., T.K., Y.K., H.E., and H.W. designed, analyzed, and interpreted the majority of experiments; B.B. provided key materials and helped interpret data and edit the manuscript; S.Y., K.Y., I.K., H.I., M.T., M.I., S.T., H.G., and T.T. provided clinical samples and helped analyze data; M.B. and K.-i.S. wrote and revised the manuscript; and K.-i.-S. conceived, designed, and supervised the whole project.

Conflict-of-interest disclosure: The authors declare no competing financial interests.

ORCID profile: M.B., 0000-0002-2347-8889.

Correspondence: Ken-ichiro Seino, Division of Immunobiology, Institute for Genetic Medicine, Hokkaido University, Kita-15, Nishi-7, Kita-ku, Sapporo 060-0815, Japan; e-mail: seino@igm.hokudai.ac.jp.

References

1. Bianchi G, Munshi NC. Pathogenesis beyond the cancer clone(s) in multiple myeloma. *Blood*. 2015;125(20):3049-3058.
2. Paiva B, van Dongen JJ, Orfao A. New criteria for response assessment: role of minimal residual disease in multiple myeloma. *Blood*. 2015;125(20):3059-3068.
3. Moreau P, Attal M, Facon T. Frontline therapy of multiple myeloma. *Blood*. 2015;125(20):3076-3084.
4. Nooka AK, Kastritis E, Dimopoulos MA, Lonial S. Treatment options for relapsed and refractory multiple myeloma. *Blood*. 2015;125(20):3085-3099.
5. Amarasekara DS, Yun H, Kim S, Lee N, Kim H, Rho J. Regulation of osteoclast differentiation by cytokine networks. *Immune Netw*. 2018;18(1):e8.
6. Lin H, Lee E, Hestir K, et al. Discovery of a cytokine and its receptor by functional screening of the extracellular proteome. *Science*. 2008;320(5877):807-811.
7. Baghdadi M, Umeyama Y, Hama N, et al. Interleukin-34, a comprehensive review. *J Leukoc Biol*. 2018;104(5):931-951.
8. Baghdadi M, Endo H, Tanaka Y, Wada H, Seino KI. Interleukin 34, from pathogenesis to clinical applications. *Cytokine*. 2017;99:139-147.
9. Chen Z, Buki K, Vääräniemi J, Gu G, Väänänen HK. The critical role of IL-34 in osteoclastogenesis. *PLoS One*. 2011;6(4):e18689.
10. Baud'huin M, Renault R, Charrier C, et al. Interleukin-34 is expressed by giant cell tumours of bone and plays a key role in RANKL-induced osteoclastogenesis. *J Pathol*. 2010;221(1):77-86.
11. Hwang SJ, Choi B, Kang SS, et al. Interleukin-34 produced by human fibroblast-like synovial cells in rheumatoid arthritis supports osteoclastogenesis. *Arthritis Res Ther*. 2012;14(1):R14.
12. Boström EA, Lundberg P. The newly discovered cytokine IL-34 is expressed in gingival fibroblasts, shows enhanced expression by pro-inflammatory cytokines, and stimulates osteoclast differentiation. *PLoS One*. 2013;8(12):e81665.
13. Dai XM, Ryan GR, Hapel AJ, et al. Targeted disruption of the mouse colony-stimulating factor 1 receptor gene results in osteopetrosis, mononuclear phagocyte deficiency, increased primitive progenitor cell frequencies, and reproductive defects. *Blood*. 2002;99(1):111-120.
14. Wang Y, Szretter KJ, Vermi W, et al. IL-34 is a tissue-restricted ligand of CSF1R required for the development of Langerhans cells and microglia. *Nat Immunol*. 2012;13(8):753-760.
15. Greter M, Lelios I, Pelczar P, et al. Stroma-derived interleukin-34 controls the development and maintenance of langerhans cells and the maintenance of microglia. *Immunity*. 2012;37(6):1050-1060.
16. Cioce M, Canino C, Goparaju C, Yang H, Carbone M, Pass HI. Autocrine CSF-1R signaling drives mesothelioma chemoresistance via AKT activation. *Cell Death Dis*. 2014;5(4):e1167.
17. Ségaliny AI, Mohamadi A, Dizier B, et al. Interleukin-34 promotes tumor progression and metastatic process in osteosarcoma through induction of angiogenesis and macrophage recruitment. *Int J Cancer*. 2015;137(1):73-85.
18. Baghdadi M, Wada H, Nakanishi S, et al. Chemotherapy-induced IL34 enhances immunosuppression by tumor-associated macrophages and mediates survival of chemoresistant lung cancer cells. *Cancer Res*. 2016;76(20):6030-6042.
19. Zhou SL, Hu ZQ, Zhou ZJ, et al. miR-28-5p-IL-34-macrophage feedback loop modulates hepatocellular carcinoma metastasis. *Hepatology*. 2016;63(5):1560-1575.
20. Franzè E, Dinallo V, Rizzo A, et al. Interleukin-34 sustains pro-tumorigenic signals in colon cancer tissue. *Oncotarget*. 2017;9(3):3432-3445.
21. Raggi C, Correnti M, Sica A, et al. Cholangiocarcinoma stem-like subset shapes tumor-initiating niche by educating associated macrophages. *J Hepatol*. 2017;66(1):102-115.
22. Baghdadi M, Endo H, Takano A, et al. High co-expression of IL-34 and M-CSF correlates with tumor progression and poor survival in lung cancers. *Sci Rep*. 2018;8(1):418.
23. Han N, Baghdadi M, Ishikawa K, et al. Enhanced IL-34 expression in nivolumab-resistant metastatic melanoma. *Inflamm Regen*. 2018;38(1):3.
24. Hofgaard PO, Jodal HC, Bommert K, et al. A novel mouse model for multiple myeloma (MOPC315.BM) that allows noninvasive spatiotemporal detection of osteolytic disease. *PLoS One*. 2012;7(12):e51892.
25. de Haart SJ, van de Donk NW, Minnema MC, et al. Accessory cells of the microenvironment protect multiple myeloma from T-cell cytotoxicity through cell adhesion-mediated immune resistance. *Clin Cancer Res*. 2013;19(20):5591-5601.
26. Zipori D. The hemopoietic stem cell niche versus the microenvironment of the multiple myeloma-tumor initiating cell. *Cancer Microenviron*. 2010;3(1):15-28.

27. Komohara Y, Noyori O, Saito Y, et al. Potential anti-lymphoma effect of M-CSFR inhibitor in adult T-cell leukemia/lymphoma. *J Clin Exp Hematop*. 2018; 58(4):152-160.

28. Baghdadi M, Ishikawa K, Endo H, et al. Enhanced expression of IL-34 in an inflammatory cyst of the submandibular gland: a case report. *Inflamm Regen*. 2018;38(1):12.

29. Catanzaro JM, Sheshadri N, Pan JA, et al. Oncogenic Ras induces inflammatory cytokine production by upregulating the squamous cell carcinoma antigens SerpinB3/B4. *Nat Commun*. 2014;5(1):3729.

30. Ancrile BB, O'Hayer KM, Counter CM. Oncogenic ras-induced expression of cytokines: a new target of anti-cancer therapeutics. *Mol Interv*. 2008;8(1): 22-27.

31. Yasmin R, Siraj S, Hassan A, Khan AR, Abbasi R, Ahmad N. Epigenetic regulation of inflammatory cytokines and associated genes in human malignancies. *Mediators Inflamm*. 2015;2015:201703.

32. Filleul O, Crompot E, Saussez S. Bisphosphonate-induced osteonecrosis of the jaw: a review of 2,400 patient cases. *J Cancer Res Clin Oncol*. 2010; 136(8):1117-1124.

33. Reid IR, Cornish J. Epidemiology and pathogenesis of osteonecrosis of the jaw. *Nat Rev Rheumatol*. 2011;8(2):90-96.

34. Sobacchi C, Schulz A, Coxon FP, Villa A, Helfrich MH. Osteopetrosis: genetics, treatment and new insights into osteoclast function. *Nat Rev Endocrinol*. 2013;9(9):522-536.